Sebastian Kühn, Joanna Freyse, Passant Atallah, Jörg Rademann, Uwe Freudenberg and Carsten Werner*

Tuning the network charge of biohybrid hydrogel matrices to modulate the release of SDF-1

https://doi.org/10.1515/hsz-2021-0175
Received February 27, 2021; accepted June 10, 2021; published online July 5, 2021

Abstract: The delivery of chemotactic signaling molecules via customized biomaterials can effectively guide the migration of cells to improve the regeneration of damaged or diseased tissues. Here, we present a novel biohybrid hydrogel system containing two different sulfated glycosaminoglycans (sGAG)/sGAG derivatives, namely either a mixture of short heparin polymers (Hep-Mal) or structurally defined nona-sulfated tetrahyaluronans (9s-HA4-SH), to precisely control the release of charged signaling molecules. The polymer networks are described in terms of their negative charge, i.e. the anionic sulfate groups on the saccharides, using two parameters, the integral density of negative charge and the local charge distribution (clustering) within the network. The modulation of both parameters was shown to govern the release characteristics of the chemotactic signaling molecule SDF-1 and allows for seamless transitions between burst and sustained release conditions as well as the precise control over the total amount of delivered protein. The obtained hydrogels with well-adjusted release profiles effectively promote MSC migration *in vitro* and emerge as promising candidates for new treatment modalities in the context of bone repair and wound healing.

Keywords: heparin; hydrogels; migration of mesenchymal stem cells (MSC); release of stromal cell-derived factor 1 (SDF-1); sulfated glycosaminoglycans (GAG); sulfated oligohyaluronan.

***Corresponding author: Carsten Werner**, Leibniz Institute of Polymer Research Dresden (IPF), Max Bergmann Center of Biomaterials Dresden (MBC), Hohe Str. 6, D-01069 Dresden, Germany; and Center for Regenerative Therapies Dresden (CRTD), Technische Universität Dresden, Fetscherstraße 105, D-01307 Dresden, Germany, E-mail: werner@ipfdd.de. https://orcid.org/0000-0003-0189-3448
Sebastian Kühn, Passant Atallah and Uwe Freudenberg, Leibniz Institute of Polymer Research Dresden (IPF), Max Bergmann Center of Biomaterials Dresden (MBC), Hohe Str. 6, D-01069 Dresden, Germany
Joanna Freyse and Jörg Rademann, Institute of Pharmacy, Medicinal Chemistry, Freie Universität Berlin, Königin-Luise-Strasse 2+4, D-14195 Berlin, Germany

Introduction

Sulfated glycosaminoglycans (sGAG) are essential components of the extracellular matrix (ECM) and are the key to many signaling processes in tissue development, homeostasis, disease and regeneration (Häcker et al. 2005; Meneghetti et al. 2015; Raman et al. 2005; Richter et al. 2018). sGAG-protein interactions are well known to be dominated by electrostatic interactions between the negatively charged GAG, containing anionic sulfate groups, and positively charged domains on the protein surface, although structural parameters such as the spatial distribution and position of ionized groups and hydrophobic interactions contribute as well (Björk and Lindahl 1982; Capila and Linhardt 2002; Garg et al. 2005; Köhling et al. 2016b; Künze et al. 2016; Panitz et al. 2016; Proudfoot et al. 2017; Walkowiak et al. 2020). The ability of sGAGs to interact with proteins in combination with powerful methodologies to study and engineer these interactions (Noti and Seeberger 2005; Turnbull 2018) has been a great inspiration for the field of biomaterials research and is fundamental to the understanding of signal transduction *in vivo*. Therefore, the incorporation of sGAG and their chemically modified derivatives into biohybrid hydrogel matrices has offered an important means to mimic the signaling properties of the ECM (Freudenberg et al. 2016; Hudalla and Murphy 2011) and develop new therapeutic approaches (Lohmann et al. 2017; Maitz et al. 2013; Thönes et al. 2019) as well as advanced tissue and disease models (Bray et al. 2015; Chwalek et al. 2014; Papadimitriou et al. 2018; Weber et al. 2017). From a physicochemical point of view, these sGAG-based polymer networks closely resemble the situation in native tissues such as GAG-assemblies or proteoglycans found within the glycocalyx of a cell or within the ECM. Here, charge carriers are not distributed homogenously but rather reside as local clusters with specific patterns represented by rather long sulfated polysaccharides, i.e. sGAG such as heparan sulfate or the closely related heparin (Richter et al. 2018). The chemoenzymatic synthesis of precisely defined short oligosaccharides and selective control over their sulfation represents a sophisticated technological approach to alter the chain length and charge distribution of sGAG, hence,

their protein binding properties (Bhattacharya et al. 2020; Yao et al. 2019). This allows for the detailed investigation of GAG-protein structure-activity relationships (Gandhi and Mancera 2008; Noti and Seeberger 2005; Xu et al. 2018) and on the other hand, can offer promising new options for the design of GAG-based hydrogel materials. Whereas the incorporation of native, long polysaccharides into 3D polymer networks corresponds to the situation within the ECM and favors 'specific' strong local interactions with spatially matching charge pairs, the usage of shorter GAG derived sulfated oligosaccharides rather results in more unspecific electrostatic interactions with charged proteins (Capila and Linhardt 2002; Garg et al. 2005; Köhling et al. 2019; Sadir et al. 2001; Walkowiak et al. 2020; Ziarek et al. 2013). This allows for a more precise and modular adjustment of charge parameters in 3D within the same material class as the intrinsic physicochemical properties of the building blocks are quite similar, being both highly sulfated carbohydrate units only differing in chain length.

Accordingly, we set out to evaluate what kind of charge distribution and interaction concept might be more powerful in modulating chemokine transport processes in biomaterials. *Concept one* describes the local clustering of charge within a polymer network enabling strong interactions with charged proteins whereas *concept two* is based on a homogeneous charge distribution within a polymer network and weaker interactions (Figure 1). In this study, the formation of hydrogels with varying charge density and distribution is achieved through the incorporation of either maleimide-functionalized heparin polysaccharides (Hep-Mal) or thiol functionalized sulfated oligohyaluronans (9s-HA4-SH) at controlled ratios into polyethylene glycol (PEG) matrices through a nearly quantitative and cytocompatible Michael type addition, a reaction scheme that has been successfully used for a recently established material platform of GAG-based biohybrid hydrogels (Atallah et al. 2018; Freudenberg et al. 2012; Limasale et al. 2020; Tsurkan et al. 2013; Zieris et al. 2014). While the heparin used in this study is a mixture of natural polysaccharides with an average of 26 highly sulfated disaccharide repeating units, 9s-HA4-SH is a much shorter tetrasaccharide chemoenzymatically derived from hyaluronan with only two chemically sulfated disaccharide repeating units, although displaying a slightly higher sulfation degree compared to heparin (Table 1). For the characterization of our material we applied a recently developed theory-driven design concept categorizing the distribution of negative charge carriers (anionic sulfate groups) within these polymer networks (Freudenberg et al. 2019). Following this quantitative approach, the sGAG content in the matrix and the sGAG sulfation pattern can be described by the following two parameters: (*P*1) the integral charge density (the number of anionic sulfate groups per hydrogel volume in [mmol/ml]) and (*P*2) the charge density on the sGAG component (the number of sulfate moieties per GAG repeating unit divided by the molecular weight of the repeating unit [mmol/(g/mol)]) which were shown to characterize the binding of strongly charged (basic or acidic) cytokines as well as the binding of weakly charged cytokines, respectively. In order to account for the different chain lengths of Hep-Mal and 9s-HA4-SH in this study, we calculated the effective (i.e. total) *P*2 of the sulfated saccharide ($P2_{\mathrm{eff}}$) by multiplying *P*2 with the number of repeating units n_{RU} so that:

$$P2_{\mathrm{eff}} = P2 * n_{\mathrm{RU}}$$

$P2_{\mathrm{eff}}$ can be seen as an extension of our previous parametric system and allows for a meaningful comparison of sGAG-based matrices containing sulfated saccharides with varying chain length without neglecting the sulfation pattern (Table 1). We consider our approach suitable for a more precise design of sGAG-based biomaterials with respect to their interaction with signaling molecules, i.e. their binding and release. In tissue development, homeostasis and disease, sGAG and their ability to reversibly bind chemokines and morphogens regulate the formation of signaling concentration gradients in the ECM to direct cell fate (Bishop et al. 2007; Parish 2006; Yan and Lin 2009; Yu et al. 2009). Therefore, the control over signaling gradients through precisely engineered sGAG-based matrices is of particular interest for both the development of new therapeutic approaches as well as more complex and realistic *in vitro* tissue and disease models (Kühn et al. 2020; Magno et al. 2020).

Stromal cell-derived factor 1 (SDF-1) also termed CXCL12, a chemokine crucial for immune cell migration, trafficking of hematopoietic stem and progenitor cells and control of angiogenic processes (Bleul et al. 1996; De Falco et al. 2004; Hattori et al. 2001; Romagnani et al. 2004), belongs to the group of strongly positively charged chemokines whose interaction with the sGAG matrices is dependent on *P*1. The protein is upregulated upon tissue injury (Ratajczak et al. 2006) and is further known to be a potent chemoattractant for mesenchymal stromal cells (MSC) (Fu et al. 2019; Honczarenko et al. 2006; Iannone et al. 2014; Son et al. 2006; Stich et al. 2009; Yu et al. 2016). MSCs, who have long been a key target for regenerative therapies (Pittenger et al. 2019; Rodríguez-Fuentes et al. 2021; Stappenbeck and Miyoshi 2009), are valuable mediators of tissue repair (Pittenger et al. 2019; Sagaradze et al. 2020) and their migration to the site of injury can be critical for successful regeneration (Kitaori et al. 2009). Consequently, engineering biomaterials that can deliver SDF-1 and guide MSC migration in a controlled and sustained

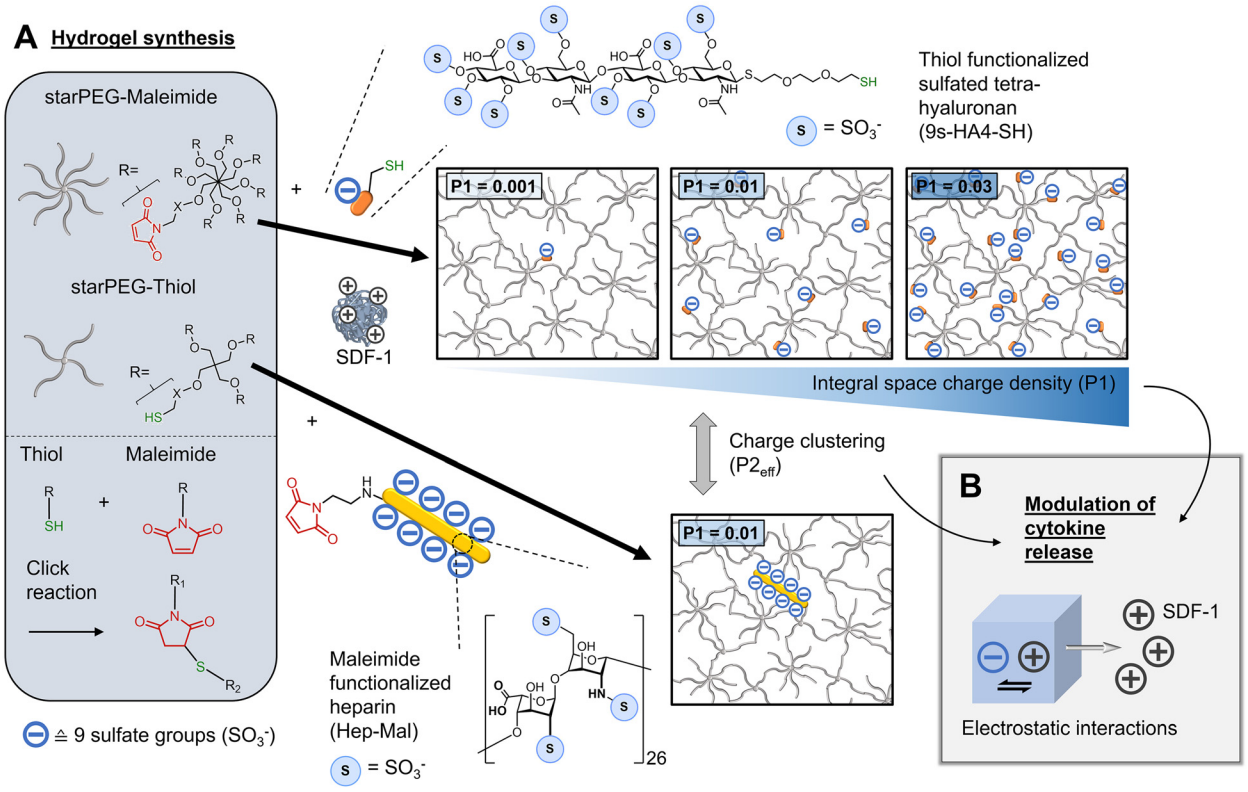

Figure 1: Synthesis of starPEG-based hydrogel matrices containing sulfated saccharides (sulfated tetrahyaluronan or polymeric heparin with an average of 26 repeating units).
(A) The hydrogel network is formed through a click reaction between thiolated 4arm starPEG and maleimide functionalized 8arm starPEG. The incorporation of thiol or maleimide mono-functionalized saccharides (9s-HA4-SH or Hep-Mal) allows for precise control over the density of sulfate groups (negative charge carriers) in the 3D hydrogel network (*P*1) and their local distribution ($P2_{eff}$) which is determined by the sulfation pattern and the chain length. (B) The (negative) charge tuning of the hydrogels can be harnessed to modulate the release of *in situ* loaded positively charged signaling molecules such as SDF-1 to stimulate healing processes and tissue regeneration.

Table 1: Chemical characteristics of GAG/GAG derivatives incorporated into the biohybrid hydrogel matrices.

Structural features	Heparin (Hep-Mal)	Sulfated tetrahyaluronan (9s-HA4-SH)
MW [g/mol]	15,000 ± 2000	1902
Sulfate groups per molecule	70	9
Disaccharide repeating units	26	2
*P*2 [mmol/(g/mol)]	4.7	5.2
$P2_{eff}$ [mmol/(g/mol)]	122	10

manner (through precisely controlled signaling gradients) may constitute a powerful tool to promote tissue regeneration processes including bone repair and wound healing. To address this challenge, we aimed at developing sGAG-based matrices with adjustable charge density and distribution to tune the release of SDF-1 and thus, stimulate and control MSC migration.

Results

Synthesis and characterization of the hydrogels with precisely controlled charge properties

The biohybrid hydrogels were formed through a Michael type addition click reaction between end-functionalized 4arm starPEG-thiol (PEG-SH) and end-functionalized 8arm starPEG-maleimide (PEG-Mal). The same reaction was harnessed to tether the mono-functionalized bioactive components into the gel where Hep-Mal was reacted with arms of the starPEG-SH while the 9s-HA4-SH was reacted to the arms of the PEG-Mal prior to the formation of the gels. The integral space charge density (*P*1) of the system was controlled through the amount of incorporated sulfated saccharides allowing for precise adjustment of *P*1 over a wide and physiologically relevant range between 0.001 and 0.03 mmol/ml (Figure 2). On the other hand, reducing

the amount of sulfated saccharide but switching from 9s-HA4-SH to Hep-Mal (longer chain but similar sulfation degree) altered the distribution of charge carriers in the network while keeping *P*1 constant (Figures 1 and 2). The molar ratio of the bioactive components (Hep-Mal and 9s-HA4-SH) to the inert PEG polymer network formers (PEG-SH and PEG-Mal) was chosen low enough to leave sufficient arms of the PEGs to ensure proper gelation, i.e. always keeping similar number of network nots via formation of covalent PEG-PEG bonds. As a result, the physical hydrogel properties – storage modulus (~2 kPa), mesh size (~12 nm) and hydrogel swelling (volumetric swelling ratio between 1 and 1.3) – are not affected by changes in the composition, i.e. the biochemical properties and thus the charging of the hydrogels can be tuned independently from the physical network properties (Figure 2). The mesh size was estimated from the storage modulus following the rubber elasticity theory (Rubinstein and Colby 2003) and 12 nm should allow for comparable diffusion of SDF-1 (hydrodynamic radius ~5 nm) (Crump et al. 1997) between the different gel types.

Modulation of the SDF-1 release through the density of negative charges (*P*1) and their distribution in the hydrogel network ($P2_{eff}$)

Next, the release of SDF-1, which was pre-loaded to the gels, was analyzed to study the effect of charge clustering and charge density on the release characteristics for the different hydrogel types. Therefore, SDF-1 (20 ng/µl gel) was added to the gel precursors prior to gelation and after successful network formation the released amount of protein was measured by ELISA in the supernatant which was completely exchanged every 24 h over a time period of seven days (Figure 3). Due to the incorporation of SDF-1 directly upon gel formation the loading efficiency of the system is considered to be 100%. The 9s-HA4-SH gels with *P*1 values of 0.28 mmol/ml (9s-HA4-SH-0.03) and 0.0093 mmol/ml (9s-HA4-SH-0.01) show a sustained linear release of about 30 and 65% of their loading within seven days, respectively (R^2 = 0.9977 and 0.9873). Furthermore, almost no burst release (<2%) was observed for the

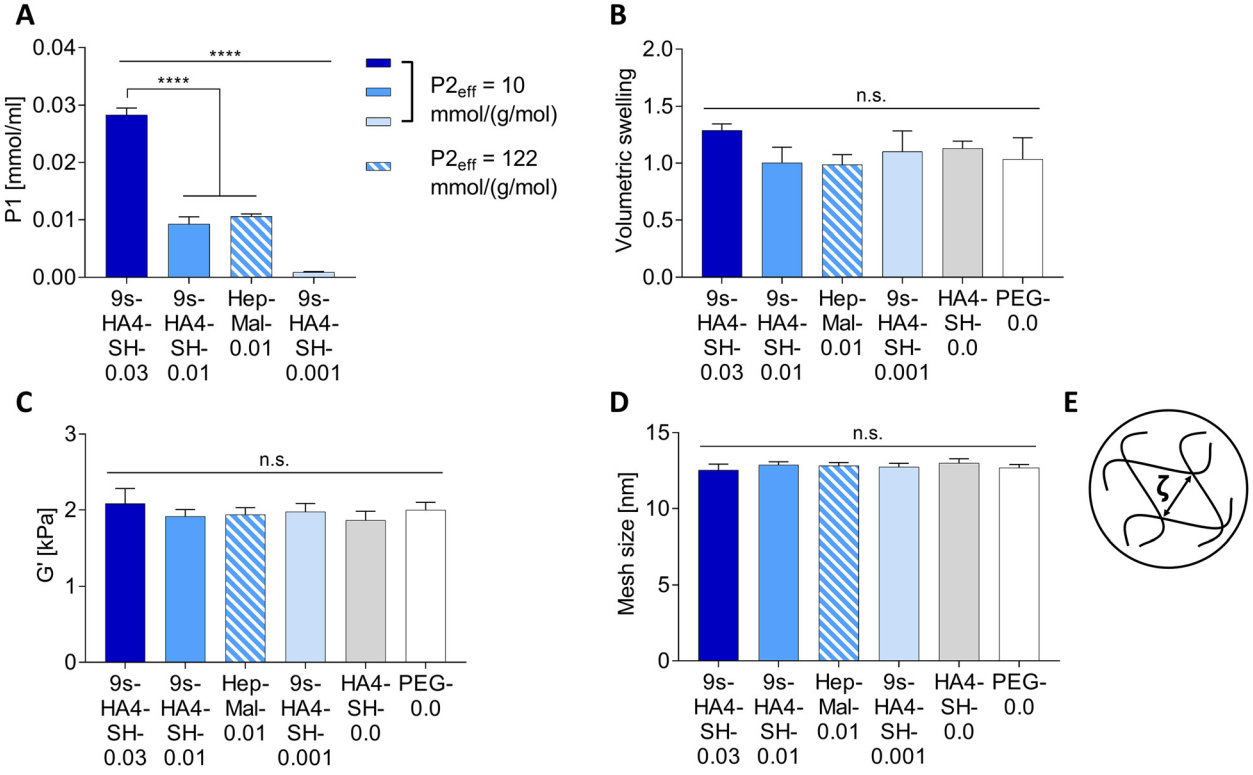

Figure 2: Biochemical and biophysical properties of the hydrogels.
(A) The integral space charge density (*P*1) of the hydrogels after equilibrium swelling. The hydrogel swelling (B), the mechanical properties (C) and the mesh size (D) remain unaffected by the modulation of the hydrogel composition. (E) Definition of the mesh size *ζ* as the distance between two crosslinks. Data shown as mean ± SD, ****$p \leq 0.0001$.

9s-HA4-SH-0.03 gels. In contrast, the gels with the lowest *P*1 of 0.00088 mmol/ml (9s-HA4-SH-0.001) present a strong burst-like characteristic and release 100% of their cargo already within four days. Over a prolonged time period a similar efficiency can be expected from the 9s-HA4-SH-0.03 and 9s-HA4-SH-0.01 gels following the linear trend of the kinetics. To further verify that the observed release kinetics can be attributed to the charge tuning the release was also analyzed for uncharged hydrogels containing either unsulfated oligohyaluronan (HA4-SH-0.0) or pure PEG gels containing no saccharide at all (PEG-0.0) and both gels release more than 50% in a 24-h burst. Overall, less than 100% release of SDF-1 is observed from the uncharged gels which indicates a stabilizing effect through complexation of SDF-1 with the sulfated saccharides where 100% of the loaded SDF-1 was released and detected (9s-HA4-SH-0.001 gels). Plotting the release of SDF-1 from the different 9s-HA4-SH hydrogels over the *P*1 of their networks revealed an exponential relationship where the release decays as the charge density (*P*1) increases (Figure 3). Due to this strong correlation, we conclude that the release of SDF-1 can be modulated through control over the *P*1 characteristic of the network. Using heparin instead of sulfated tetrahyaluronan a more clustered presentation of charges in the gel network is achieved while keeping *P*1 comparable. The charge clustering has a dramatic effect on the release of SDF-1 as most release takes place within the early time points for the Hep-Mal-0.01 gels as compared to a linear release of the 9s-HA4-SH-0.01 gels. Furthermore, a large portion of SDF-1 (~65% after seven days) is retained much longer within the Hep-Mal-0.01 hydrogels and the total released protein after seven days is significantly lower (Figure 3). This demonstrates that the diffusion of SDF-1 and potentially also other strongly charged proteins in GAG-based matrices is not only governed by *P*1. Instead, the distribution of charge carriers and local clustering might be a valuable parameter to consider when engineering GAG-based biomaterials and other charged hydrogel matrices for the release of signaling molecules.

Control over MSC migration through SDF-1 release from the hydrogels

In order to assess the cell guiding properties of the biohybrid hydrogels, MSC migration was measured in a transwell setup. For this purpose, 9s-HA4-SH-0.001 and 9s-

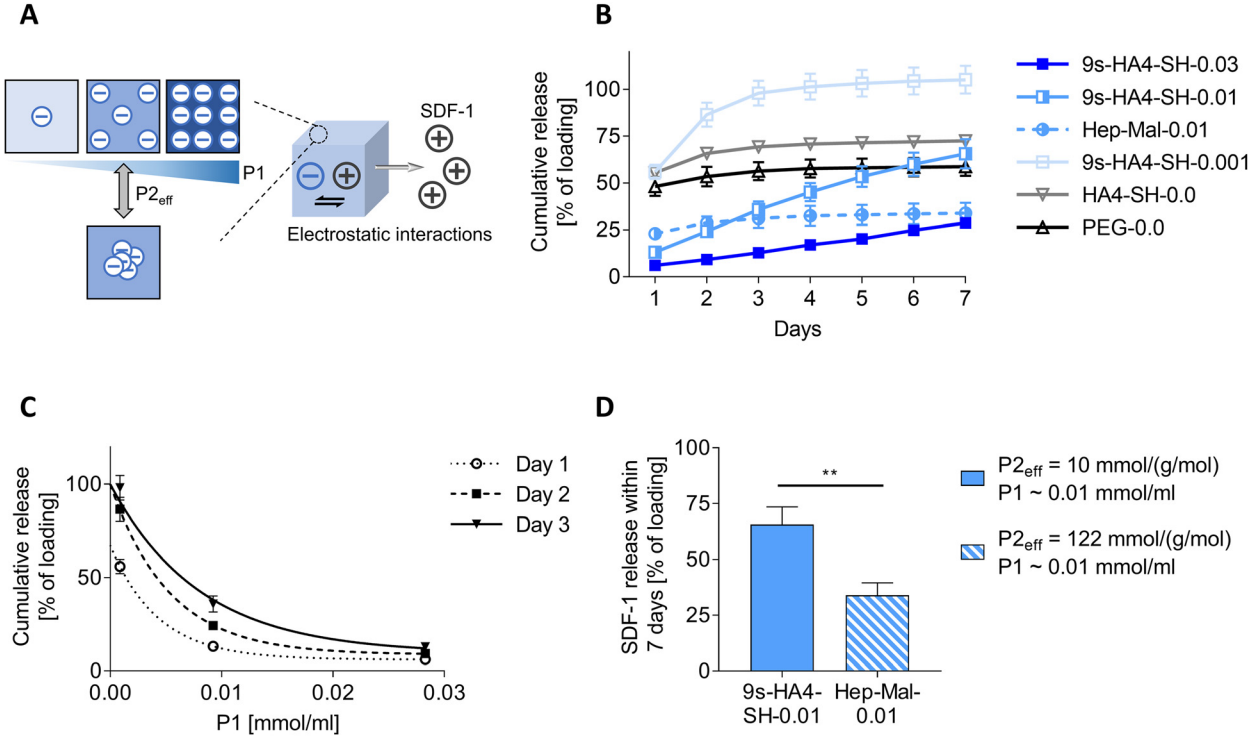

Figure 3: Tunable SDF-1 release from the hydrogels with different charge characteristics.
(A) Schematic representation of the two parameters *P*1 and $P2_{eff}$ that govern the release of SDF-1 from GAG-based hydrogels with different charge density and distribution. (B) Experimentally determined cumulative protein release from hydrogels loaded with SDF-1. (C) SDF-1 release as a function of *P*1 for 9s-HA4-SH gels and the least squares best fits of the data using an exponential decay model. (D) Effect of $P2_{eff}$ on the release of SDF-1. Data is shown as mean ± SD, $^{**}p \leq 0.005$.

HA4-SH-0.01 hydrogels were chosen as they represent the most effective release system and display very distinct profiles, i.e. burst vs. sustained release. The SDF-1 loaded hydrogels were incubated with cell culture medium over a period of six days (medium exchange every second day) and the chemotactic effect of the supernatant collected at the different time points was quantified (Figure 4). The SDF-1 concentration required to stimulate MSC migration was previously determined (data not shown). A higher loading of the 9s-HA4-SH-0.01 hydrogels (65 ng/µl gel) compared to 9s-HA4-SH-0.001 hydrogels (18 ng/µl gel) was chosen to yield a comparable total release of SDF-1 for both gel types within the first two days based on the release profiles determined by ELISA. Overall, the different release characteristics of the two gel types are well reflected in the migratory behavior of MSCs. In response to the supernatant collected after the first two days the migration is comparable between both gel types and a similar level is maintained by the 9s-HA4-SH-0.01 gels also for the later time points as they continue to release SDF-1 at a similar rate. In contrast, the SDF-1 concentration in the supernatant collected from 9s-HA4-SH-0.001 gels at day four and six is not further sufficient to induce a significant cell response since the hydrogels have released most of their cargo already at day two. These results clearly show that the modulation of release profiles (burst vs. sustained release) by means of *P*1 can be directly translated to the cellular level in order to fine-tune the cell-instructive properties of the system.

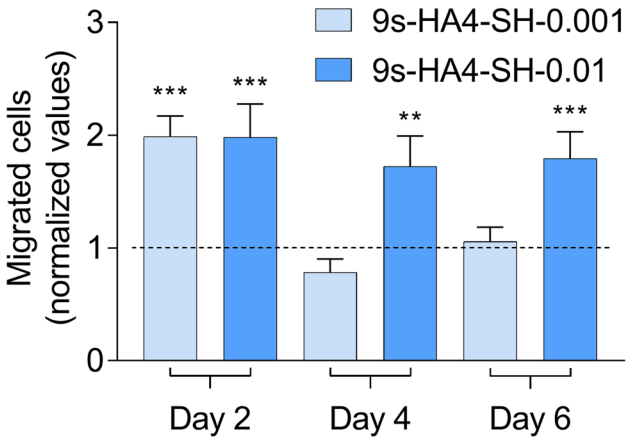

Figure 4: Analysis of the cell guiding properties of the biohybrid hydrogels.
Transwell MSC migration in response to SDF-1 released from hydrogels containing sulfated tetrahyaluronan. The hydrogel loading was adjusted to yield the same level of SDF-1 release within the first two days and release medium was exchanged in two-day intervals. Values are normalized to the negative control containing no SDF-1. Data shown as mean ± SD, Statistical comparison to the negative control (dashed line), $^{**}p \leq 0.01$, $^{***}p \leq 0.001$.

Discussion

We have developed a sGAG-based hydrogel system that allows for a flexible adjustment of the density and distribution of negative charge within the polymer network. Our approach bridges, for the first time, two very different concepts of charge distribution (clustered vs. homogeneous) in these polymer networks with fundamental impacts for the binding and release of charged proteins. In native tissue, i.e. within the ECM or the glycocalyx of cells, sGAG act as critical mediators of many signaling processes and due to their anionic sulfate groups, introduce strong clusters of negative charge that constitute the dominating driving force for the interaction with charged signaling molecules. This aspect (concept one) is captured by ECM-mimicking biomaterials through the incorporation of sulfated polysaccharides that are sufficiently long to allow for strong electrostatic complexation of proteins, i.e. native or chemically modified sGAG such as heparan sulfate or, in our case, its related form heparin (Hep-Mal). Opposed to the situation in native tissue, the second scenario (concept two) provides a much more homogenous charge distribution in the polymer matrix which we achieved by integrating chemoenzymatically synthesized short sulfated oligosaccharides, namely sulfated tetrahyaluronan (9s-HA4-SH). Both gel variants can be described with respect to their integral space charge density *P*1, following our previously established quantitative approach for the rational design of such materials (Freudenberg et al. 2019), and the effect of charge clustering can be expressed as the newly defined parameter $P2_{eff}$ (Figure 1). Thanks to the modular nature of the Michael type addition the concentration of thiol- or maleimide functionalized sulfated saccharides within the PEG matrices is easily adjusted to yield a wide range of charge densities *P*1. Furthermore, it allows for seamless switching between the two concepts of charge distribution, i.e. clustered and homogeneous, by simply exchanging the sulfated carbohydrates, i.e. heparin and sulfated tetrahyaluronan, respectively. In agreement with our previous study on protein binding (Freudenberg et al. 2019) we were able to interpret our release data in terms of *P*1 and show a strong relationship between *P*1 and the release of SDF-1 using 9s-HA4-SH gels (*concept two*). The charge tuning of the matrices did not affect their biophysical properties (mesh size and storage modulus) rendering them a very flexible material platform since the decoupled properties can be customized and adjusted independently to fit specific applications. With up to

100% release the system proofs extremely effective and the sustained linear kinetics of the 9s-HA4-SH-0.01 and 9s-HA4-SH-0.03 gels allow for precise predictions greatly improving its robustness and technical manageability.

This is all the more important since the modulation of protein release can be directly translated into cell-instructive signaling as demonstrated by the MSC migration experiments, with exact control over the duration and intensity of the signal. Furthermore, the migration assay demonstrates the feasibility of the approach to promote MSC migration through SDF-1 release and renders the material a promising candidate for new treatment modalities to support endogenous tissue regeneration. Furthermore, since SDF-1 was also shown to mediate the homing of transplanted MSCs (Vanden Berg-Foels 2014) our material could represent an interesting option for improving the outcome of stem cell-based therapies. Regarding a broader applicability of our material, a similar release behavior of other important signaling molecules that are strongly charged such as VEGF-A, IFNγ, bNGF or IL-8 can be expected since consistent trends were observed regarding the binding to sGAG-based matrices (Freudenberg et al. 2019). Although the comparison of binding and release characteristics executed in this study for one single protein captures only a part of the picture, the consistent trends point towards a broader validity of the developed approach to modulate protein interactions with negatively charged hydrogel matrices.

The distribution of charge carriers within the network was controlled through $P2_{eff}$ as an expression of the sulfate group density on the saccharide ($P2$) and the length of the carbohydrate. Keeping $P1$ constant and comparing gels with locally accumulated charge carriers (Hep-Mal gels – concept one) and gels with a more homogeneous presentation (9s-HA4-SH gels – concept two) demonstrates the importance of charge distribution in the network. Charge clustering in the case of heparin results in overall slower release of SDF-1 and longer retention within the gel which was to be expected from comparable gel systems showing similar release kinetics as well as faster and higher release of SDF-1 upon degradation of the material (Prokoph et al. 2012; Spiller et al. 2019). The observed effects of charge clustering on SDF-1 release further coincide with the binding strength of SDF-1 for the sulfated saccharides. Besides structural parameters such as the position of the sulfate groups on the saccharide, the interaction strength of SDF-1 and other regulatory proteins was shown to be determined by the number of sulfate groups ($P2$) and the length of the carbohydrate, hence $P2_{eff}$, resulting in significantly stronger binding for longer sulfated carbohydrates (Köhling et al. 2019; Sadir et al. 2001). The ability to chemically define $P2$ and the position of the sulfate groups independent of the length of the sulfated saccharide (Köhling et al. 2019; Zieris et al. 2014) emphasizes the potential of our system to control and fine-tune the release profiles of charged proteins. Although specific interactions and entropic effects such as the formation of higher order structures should not be neglected for sGAG-protein interaction (Capila and Linhardt 2002; Garg et al. 2005; Köhling et al. 2016b; Künze et al. 2016; Proudfoot et al. 2017; Walkowiak et al. 2020) the observed trends underline the major role of electrostatic interactions and support the validity/robustness of our charge-oriented approach as well as the relevance of $P2_{eff}$ as a measure of charge clustering. However, regarding the design of sulfated saccharides for hydrogel materials, a persisting question concerns the transition between the two regimes of $P2_{eff}$ at which the interaction of sulfated saccharides with a protein is either strong and involves specific binding sites on the protein (concept one) or rather weak and non-specific (concept two). Here, thermodynamic analysis and molecular modelling of GAG-protein interactions represent powerful tools to determine the physicochemical properties of a given saccharide (chain length, $P2$ and sulfate group position) that allow for proper binding of specific proteins and thus, to distinguish the two cases (Köhling et al. 2019; Sadir et al. 2001; Walkowiak et al. 2020). Such analysis for SDF-1 clearly shows that heparin falls in the first category of strong 'specific' binding if a critical threshold of 12–14 monosaccharide units is reached (Sadir et al. 2001). Even though the sulfate group density ($P2$) of the tetrahyaluronan is slightly higher compared to heparin, the molecule exhibits only half the number of monosaccharide units required for strong binding to heparin and therefore, is likely to belong to the second category. This is reflected in the affinity constants found in the literature determined by fluorescence polarization assays (Köhling et al. 2019; Ziarek et al. 2013) measuring a 100-fold lower K_D value for SDF-1 binding to heparin compared to sulfated tetrahyaluronan, although it has to be pointed out that the two carbohydrates have not been directly compared in the same study. Altogether, our results clearly demonstrate that the density as well as the distribution of charge carriers within sGAG-based matrices can be utilized to control the release of strongly charged proteins.

Concept two, a homogeneous charge distribution that introduces more uniform non-specific electrostatic interactions, promotes sustained release of charged proteins such as SDF-1 with an excellent degree of control and 100% effectiveness. This points to the importance of both

parameters, $P1$ and $P2_{eff}$, for the superior release kinetics that have been observed. As such, reducing clustered charges going hand in hand with a more homogenous charge distribution within the polymer network weakens the possibilities for local 'snap in'-formations of strong ion pairs. This may lead to a seamless transition between global ($P1$) and local ($P2_{eff}$) related effects. This finding will help to more quantitatively describe the interplay of both parameters allowing for an even more precise tuning of protein-network interactions.

The obtained results are promising from a therapeutic point of view and for the engineering of signaling gradients in artificial tissue constructs. Precise and gradual modulation of protein supply and transport in engineered matrices becomes increasingly important for the development of more sophisticated and multifunctional material systems that better account for the structural and functional complexity of living tissue and provide the intricate cues for successful development *in vitro* (Kühn et al. 2020; Magno et al. 2020). However, tissue engineering and regenerative medicine not only requires release systems for soluble mediators but also a supportive scaffold for cells. Considering the fact that sGAG determine the presentation and thus the function of proteins through site-specific binding (Häcker et al. 2005; Handel et al. 2005; Meneghetti et al. 2015; Panitz et al. 2016; Proudfoot et al. 2017; Raman et al. 2005), local strong interactions with proteins, closely mimicking the situation in the native ECM as in *concept one* (Hep-Mal gels), are crucial for a successful matrix design (Freudenberg et al. 2016). Accordingly, several tissue and disease models have been developed using comparable heparin-based hydrogels (Bray et al. 2015; Chwalek et al. 2014; Tsurkan et al. 2013; Weber et al. 2017).

In conclusion, concept one and concept two can be considered complementary approaches in the design of cell-instructive materials for tissue engineering and regenerative medicine and switching from one regime to the other within the same material class by means of $P2_{eff}$ underlines the versatility of our approach. In order to fully establish $P2_{eff}$ as an expansion of our design concept and proof a more general applicability, future studies should systematically investigate the matrix-protein interactions in terms of $P1$, $P2$ and $P2_{eff}$ for a broader range of proteins and additional matrix systems. In particular, fully synthetic sGAG analogs based on sulfonated polymers have started to emerge as valuable alternatives to native sGAG/sGAG derivatives (Paluck et al. 2016). In synergy with a charge-based material design that is able to account for their structural diversity these sGAG mimetic polymers are envisioned to provide unprecedented options for the matrix-mediated control over transport and presentation of signaling molecules.

Materials and methods

Synthesis of maleimide functionalized heparin

Maleimide functionalized heparin was synthesized in-house following a previously established protocol (Tsurkan et al. 2013) where the molar ratio to heparin was reduced to achieve mono functionalization. Briefly, in an ice bath 100 mg of the heparin (Merck, Germany) were dissolved in 540 µl ultrapure water followed by the addition of 40 µl of 144 mg/ml 1-ethyl-3-(3-dimethylaminopropyl) carbodiimide (EDC) and 80 µl of 41 mg/ml N-hydroxysulfosuccinimide (s-NHS) (Sigma-Aldrich, USA). The reaction was allowed to proceed for 20 min before adding 40 µl of 95 mg/ml of N-(2-aminoethyl) maleimide. The mixture was allowed to react overnight with continuous stirring at room temperature. Finally, the reaction mixture was dialyzed (molecular weight cutoff MWCO = 8 kDa) against 1 M NaCl for one day and then against deionized water for another day, concentrated, and lyophilized.

Synthesis of thiol functionalized oligohyaluronans

Sulfated glycosyl thiol (9s-HA4-SH) was synthesized in a six-step synthesis starting from tetrahyaluronan-1-thiobenzoate (HA4-SBz) as previously described (Köhling et al. 2016a,b, 2019). In short, after saponification of the tetrahyaluronan-1-thiobenzoate, the *in situ* generated glycosyl thiolate was alkylated with 2-[2-[2-[(triphenylmethyl)-thio]-ethoxy-ethoxy]-ethyl]-bromide to give a hyaluronan-tetrasaccharide HA4-S-PEG-STrt, that was conjugated with an S-trityl-protected polyethylene linker. After acidic deprotection of the S-trityl group the resulting free thiol was oxidized to the dimeric disulfide (HA4-S-PEG-S-)$_2$ under basic conditions (0.1 M NaOH) under constant air bubbling. Sulfation of the free hydroxyl groups using SO_3·pyridin-complex in DMF and purification over dialysis (MWCO = 1 kDa) gave the bivalent octadeca-sulfo-disulfide (9s-HA4-S-PEG-S-)$_2$. The disulfide was treated with an access of tris(2-carboxyethyl)phosphine (TCEP) in degassed water to release the free thiol functionalized tetrahyaluronan (9s-HA4-SH) in 26% yield over all steps.

The unsulfated tetrahyaluronan-1-thiol (HA4-SH) was synthesized from the hyaluronan tetrasaccharide conjugated with an S-trityl-protected polyethylene linker HA4-S-PEG-STrt. After acidic deprotection of the S-trityl group to the free thiol, the product HA4-SH was purified over HPLC (H_2O/AcCN) 95:5 within 20 min to 70:30) and isolated in 72% yield.

Hydrogel synthesis and characterization

Hydrogel formation was achieved by dissolving the maleimide end-functionalized 8arm starPEG (JenKem, USA, 20,000 g/mol) and the thiol end-functionalized 4arm starPEG (JenKem 10,000 g/mol) in sterile

PBS at a molar ratio of 1:1 (solid content = 3% (w/v)). To incorporate the sulfated saccharides into the hydrogels, 9s-HA4-SH was added to the 8arm starPEG-Mal solution whereas Hep-Mal was added to the 4arm starPEG-SH solution. The ratio of sulfated saccharide to the respective PEG was chosen to yield the final *P*1 values of the hydrogels.

Storage moduli of the free-standing hydrogel materials were determined by rotational rheometry. Mechanical properties of hydrogel discs were measured with 25 mm parallel plate geometry in an Ares LN2 (TA Instruments, Germany). The frequency sweeps were carried out at a shear frequency range from 10^{-1} rad s^{-1} to 10^{2} rad s^{-1} with strain amplitude of 2%. Mean values of the storage modulus were calculated. Experiments were performed in triplicate. The gel volumetric swelling of the swollen hydrogel disks was determined by the following equation:

$$Q = \left(\frac{d}{d_0}\right)^3$$

where d_0 is the initial diameter of the unswollen gel disk and d is the final diameter of the gel disk swollen for 24 h in PBS. The hydrogel mesh size ζ was estimated from the storage modulus G' of the hydrogels based on the rubber elasticity theory (Rubinstein and Colby 2003) using the following equation:

$$\zeta = \left(\frac{G' N_A}{RT}\right)^{-\frac{1}{3}}$$

where N_A is the Avogadro constant, R is the molar gas constant and T is the temperature.

Characterization of the charge density and distribution in terms of *P*1, *P*2 and $P2_{eff}$

The concentration of sulfate groups in the hydrogels after equilibrium swelling *P*1 was calculated as follows:

$$P1 = \frac{n_{\text{sulfate}_{\text{total}}} * c_{\text{Saccharide}}}{Q}$$

where $n_{\text{sulfate}_{\text{total}}}$ is the total number of sulfate groups per saccharide molecule, $c_{\text{saccharide}}$ is the saccharide concentration in the unswollen gels and Q is the volumetric swelling factor.

The density of sulfate groups on the individual saccharide molecules *P*2 and $P2_{\text{eff}}$ were determined using the following equation:

$$P2 = \frac{n_{\text{sulfate}_{\text{RU}}}}{MW_{\text{RU}}}$$

and:

$$P2_{\text{eff}} = P2 * n_{\text{RU}}$$

where $n_{\text{sulfate}_{\text{RU}}}$ is the number of sulfate groups per disaccharide repeating unit, MW_{RU} is the molecular weight of the repeating unit and n_{RU} is the number of repeating units per saccharide molecule.

Quantification of SDF-1 release from the hydrogels

For the release studies SDF-1 (PeproTech, USA) was added to the precursor solutions (containing the GAG component) prior to gelation and 10 µl gels containing 20 ng/µl SDF-1 were casted at the bottom of a 0.5 ml reaction tube. The gels were incubated at RT with 400 µl PBS and the supernatant was collected and replaced every 24 h. Collected supernatant was stored at −80 °C for subsequent ELISA (R&D systems, USA) to determine the SDF-1 release.

Isolation of primary MSCs

Human primary bone marrow MSCs were isolated from bone marrow aspirates of healthy male donors aged between 20 and 30 years after obtaining informed consent. Primary MSCs were expanded and characterized as described previously (Oswald et al. 2004). Cells were maintained in a humidified atmosphere of 5% CO_2 in low-glucose Dulbecco's modified Eagle medium (DMEM, Gibco, USA) supplemented with 10% fetal bovine serum (FBS, Gibco) and penicillin/streptomycin (1000 Units/ml each, Gibco). Medium was changed every two to three days and cells were expanded until passage three.

Cell migration assay

For cell migration studies 9s-HA4-SH-0.01 and 9s-HA4-SH-0.001 hydrogels were loaded with SDF-1 (65 and 18 ng/µl gel, respectively) so that both gel types release a comparable amount of SDF-1 within the first two days based on the release experiments. The SDF-1 loaded hydrogels were incubated with complete medium (DMEM, Gibco containing 10% FBS) at RT, the supernatant was collected every second day and stored at −80 °C for the migration experiments. The migratory response of MSCs was compared to complete medium containing 150 ng/ml SDF-1 and complete medium without SDF-1 according to a previously used protocol (Aliperta et al. 2017). In short, 1×10^5 bone marrow derived MSCs were seeded in transwell inserts (Sarstedt, Germany, TC inserts, 8 µm pore size), the inserts were added to a 24-well plate containing the SDF-1 samples and incubated in normoxic incubator for 20 h at 37 °C. Subsequently, the cells from the top side of the membrane insert were removed and migrated cells on the bottom side of the membrane were fixed with 4% formaldehyde (Sigma-Aldrich), stained with 1% crystal violet (Sigma-Aldrich) and then visualized using a Zeiss Axiovert 40 CFL microscope equipped with an AxioCam HR camera (both Zeiss, Germany).

Statistical analysis

All statistics were performed using GraphPad Prism 7 (GraphPad Software Inc.). All values are reported as mean ± standard deviation for at least three-independent samples. Where indicated statistical analysis was performed using a two-tailed *t*-test or one-way analysis of variance (ANOVA) followed by a Tukey's post hoc test with a 95% confidence interval.

Acknowledgments: We thank Dr. Hartmut Komber (IPF Dresden) for ^{1}H NMR measurements and Dagmar Pette for her excellent technical assistance.

Author contributions: All the authors have accepted responsibility for the entire content of this submitted manuscript and approved submission.

Research funding: This work has been supported by the DFG German Research Council (SFB-TRR 67: A8 and A 10).
Conflict of interest statement: The authors declare no conflicts of interest regarding this article.

References

Aliperta, R., Welzel, P.B., Bergmann, R., Freudenberg, U., Berndt, N., Feldmann, A., Arndt, C., Koristka, S., Stanzione, M., Cartellieri, M., et al. (2017). Cryogel-supported stem cell factory for customized sustained release of bispecific antibodies for cancer immunotherapy. Sci. Rep. 7: 1–16.

Atallah, P., Schirmer, L., Tsurkan, M., Putra Limasale, Y.D., Zimmermann, R., Werner, C., and Freudenberg, U. (2018). In situ-forming, cell-instructive hydrogels based on glycosaminoglycans with varied sulfation patterns. Biomaterials 181: 227–239.

Bhattacharya, D.S., Svechkarev, D., Bapat, A., Patil, P., Hollingsworth, M.A., and Mohs, A.M. (2020). Sulfation modulates the targeting properties of hyaluronic acid to P-selectin and CD44. ACS Biomater. Sci. Eng. 6: 3585–3598.

Bishop, J.R., Schuksz, M., and Esko, J.D. (2007). Heparan sulphate proteoglycans fine-tune mammalian physiology. Nature 446: 1030–1037.

Björk, I. and Lindahl, U. (1982). Mechanism of the anticoagulant action of heparin. Mol. Cell. Biochem. 48: 161–182.

Bleul, C.C., Fuhlbrigge, R.C., Casasnovas, J.M., Aiuti, A., and Springer, T.A. (1996). A highly efficacious lymphocyte chemoattractant, stromal cell-derived factor 1 (SDF-1). J. Exp. Med. 184: 1101–1109.

Bray, L.J., Binner, M., Holzheu, A., Friedrichs, J., Freudenberg, U., Hutmacher, D.W., and Werner, C. (2015). Multi-parametric hydrogels support 3D invitro bioengineered microenvironment models of tumour angiogenesis. Biomaterials 53: 609–620.

Capila, I. and Linhardt, R.J. (2002). Heparin-protein interactions. Angew. Chem. Int. Ed. 41: 390–412.

Chwalek, K., Tsurkan, M.V., Freudenberg, U., and Werner, C. (2014). Glycosaminoglycan-based hydrogels to modulate heterocellular communication in in vitro angiogenesis models. Sci. Rep. 4: 4–11.

Crump, M.P., Gong, J.-H., Loetscher, P., Rajarathnam, K., Amara, A., Arenzana-Seisdedos, F., Virelizier, J.-L., Baggiolini, M., Sykes, B.D., and Clark-Lewis, I. (1997). Solution structure and basis for functional activity of stromal cell-derived factor-1; dissociation of CXCR4 activation from binding and inhibition of HIV-1. EMBO J. 16: 6996–7007.

De Falco, E., Porcelli, D., Torella, A.R., Straino, S., Iachininoto, M.G., Orlandi, A., Truffa, S., Biglioli, P., Napolitano, M., Capogrossi, M.C., et al. (2004). SDF-1 involvement in endothelial phenotype and ischemia-induced recruitment of bone marrow progenitor cells. Blood 104: 3472–3482.

Freudenberg, U., Atallah, P., Limasale, Y.D.P., and Werner, C. (2019). Charge-tuning of glycosaminoglycan-based hydrogels to program cytokine sequestration. Faraday Discuss 219: 244–251.

Freudenberg, U., Liang, Y., Kiick, K.L., and Werner, C. (2016). Glycosaminoglycan-based biohybrid hydrogels: a sweet and smart choice for multifunctional biomaterials. Adv. Mater. 28: 8861–8891.

Freudenberg, U., Sommer, J.U., Levental, K.R., Welzel, P.B., Zieris, A., Chwalek, K., Schneider, K., Prokoph, S., Prewitz, M., Dockhorn, R., et al. (2012). Using mean field theory to guide biofunctional materials design. Adv. Funct. Mater. 22: 1391–1398.

Fu, Liu, Halim, Ju, Luo, and Song (2019). Mesenchymal stem cell migration and tissue repair. Cells 8: 784.

Gandhi, N.S. and Mancera, R.L. (2008). The structure of glycosaminoglycans and their interactions with proteins. Chem. Biol. Drug Des. 72: 455–482.

Garg, H.G., Linhardt, R.J., and Hales, C.A. (Eds.) (2005). Chemistry and biology of heparin and heparan sulfate. In: *Chemistry and biology of heparin and heparan sulfate*. Elsevier, Oxford.

Häcker, U., Nybakken, K., and Perrimon, N. (2005). Heparan sulphate proteoglycans: the sweet side of development. Nat. Rev. Mol. Cell Biol. 6: 530–541.

Handel, T.M., Johnson, Z., Crown, S.E., Lau, E.K., Sweeney, M., and Proudfoot, A.E. (2005). Regulation of protein function by glycosaminoglycans - as exemplified by chemokines. Annu. Rev. Biochem. 74: 385–410.

Hattori, K., Heissig, B., Tashiro, K., Honjo, T., Tateno, M., Shieh, J.H., Hackett, N.R., Quitoriano, M.S., Crystal, R.G., Rafii, S., et al. (2001). Plasma elevation of stromal cell-derived factor-1 induces mobilization of mature and immature hematopoietic progenitor and stem cells. Blood 97: 3354–3360.

Honczarenko, M., Le, Y., Swierkowski, M., Ghiran, I., Glodek, A.M., and Silberstein, L.E. (2006). Human bone marrow stromal cells express a distinct set of biologically functional chemokine receptors. Stem Cell. 24: 1030–1041.

Hudalla, G.A. and Murphy, W.L. (2011). Biomaterials that regulate growth factor activity via bioinspired interactions. Adv. Funct. Mater. 21: 1754–1768.

Iannone, M., Ventre, M., Pagano, G., Giannoni, P., Quarto, R., and Netti, P.A. (2014). Defining an optimal stromal derived factor-1 presentation for effective recruitment of mesenchymal stem cells in 3D. Biotechnol. Bioeng. 111: 2303–2316.

Kitaori, T., Ito, H., Schwarz, E.M., Tsutsumi, R., Yoshitomi, H., Oishi, S., Nakano, M., Fujii, N., Nagasawa, T., and Nakamura, T. (2009). Stromal cell-derived factor 1/CXCR4 signaling is critical for the recruitment of mesenchymal stem cells to the fracture site during skeletal repair in a mouse model. Arthritis Rheum. 60: 813–823.

Köhling, S., Blaszkiewicz, J., Ruiz-Gómez, G., Fernández-Bachiller, M.I., Lemmnitzer, K., Panitz, N., Beck-Sickinger, A.G., Schiller, J., Pisabarro, M.T., and Rademann, J. (2019). Syntheses of defined sulfated oligohyaluronans reveal structural effects, diversity and thermodynamics of GAG-protein binding. Chem. Sci. 10: 866–878.

Köhling, S., Exner, M.P., Nojoumi, S., Schiller, J., Budisa, N., and Rademann, J. (2016a). One-pot synthesis of unprotected anomeric glycosyl thiols in water for glycan ligation reactions with highly functionalized sugars. Angew. Chem. Int. Ed. 55: 15510–15514.

Köhling, S., Künze, G., Lemmnitzer, K., Bermudez, M., Wolber, G., Schiller, J., Huster, D., and Rademann, J. (2016b). Chemoenzymatic synthesis of nonasulfated tetrahyaluronan with a paramagnetic tag for studying its complex with interleukin-10. Chem. Eur J. 22: 5563–5574.

Kühn, S., Sievers, J., Stoppa, A., Träber, N., Zimmermann, R., Welzel, P.B., and Werner, C. (2020). Cell-instructive multiphasic gel-in-gel materials. Adv. Funct. Mater. 30: 1908857.

Künze, G., Köhling, S., Vogel, A., Rademann, J., and Huster, D. (2016). Identification of the glycosaminoglycan binding site of interleukin-10 by NMR spectroscopy. J. Biol. Chem. 291: 3100–3113.

Limasale, Y.D.P., Atallah, P., Werner, C., Freudenberg, U., and Zimmermann, R. (2020). Tuning the local availability of VEGF within glycosaminoglycan-based hydrogels to modulate vascular endothelial cell morphogenesis. Adv. Funct. Mater. 30: 2000068.

Lohmann, N., Schirmer, L., Atallah, P., Wandel, E., Ferrer, R.A., Werner, C., Simon, J.C., Franz, S., and Freudenberg, U. (2017). Glycosaminoglycan-based hydrogels capture inflammatory chemokines and rescue defective wound healing in mice. Sci. Transl. Med. 9, https://doi.org/10.1126/scitranslmed.aai9044.

Magno, V., Meinhardt, A., and Werner, C. (2020). Polymer hydrogels to guide organotypic and organoid cultures. Adv. Funct. Mater. 30: 2000097.

Maitz, M.F., Freudenberg, U., Tsurkan, M.V., Fischer, M., Beyrich, T., and Werner, C. (2013). Bio-responsive polymer hydrogels homeostatically regulate blood coagulation. Nat. Commun. 4: 1–7.

Meneghetti, M.C., Hughes, A.J., Rudd, T.R., Nader, H.B., Powell, A.K., Yates, E.A., and Lima, M.A. (2015). Heparan sulfate and heparin interactions with proteins. J. R. Soc. Interface 12: 20150589.

Noti, C. and Seeberger, P.H. (2005). Chemical approaches to define the structure-activity relationship of heparin-like glycosaminoglycans. Chem. Biol. 12: 731–756.

Oswald, J., Boxberger, S., Jørgensen, B., Feldmann, S., Ehninger, G., Bornhäuser, M., and Werner, C. (2004). Mesenchymal stem cells can be differentiated into endothelial cells in vitro. Stem Cell. 22: 377–384.

Paluck, S.J., Nguyen, T.H., and Maynard, H.D. (2016). Heparin-mimicking polymers: synthesis and biological applications. Biomacromolecules 17: 3417–3440.

Panitz, N., Theisgen, S., Samsonov, S.A., Gehrcke, J.P., Baumann, L., Bellmann-Sickert, K., Köhling, S., Teresa Pisabarro, M., Rademann, J., Huster, D., et al. (2016). The structural investigation of glycosaminoglycan binding to CXCL12 displays distinct interaction sites. Glycobiology 26: 1209–1221.

Papadimitriou, C., Celikkaya, H., Cosacak, M.I., Mashkaryan, V., Bray, L., Bhattarai, P., Brandt, K., Hollak, H., Chen, X., He, S., et al. (2018). 3D culture method for Alzheimer's disease modeling reveals interleukin-4 rescues Aβ42-induced loss of human neural stem cell plasticity. Dev. Cell 46: 85–101.

Parish, C.R. (2006). The role of heparan sulphate in inflammation. Nat. Rev. Immunol. 6: 633–643.

Pittenger, M.F., Discher, D.E., Péault, B.M., Phinney, D.G., Hare, J.M., and Caplan, A.I. (2019). Mesenchymal stem cell perspective: cell biology to clinical progress. NPJ Regen. Med. 4: 1–15.

Prokoph, S., Chavakis, E., Levental, K.R., Zieris, A., Freudenberg, U., Dimmeler, S., and Werner, C. (2012). Sustained delivery of SDF-1α from heparin-based hydrogels to attract circulating pro-angiogenic cells. Biomaterials 33: 4792–4800.

Proudfoot, A.E.I., Johnson, Z., Bonvin, P., and Handel, T.M. (2017). Glycosaminoglycan interactions with chemokines add complexity to a complex system. Pharmaceuticals 10: 70.

Raman, R., Sasisekharan, V., and Sasisekharan, R. (2005). Structural Insights into biological roles of protein-glycosaminoglycan interactions. Chem. Biol. 12: 267–277.

Ratajczak, M.Z., Zuba-Surma, E., Kucia, M., Reca, R., Wojakowski, W., and Ratajczak, J. (2006). The pleiotropic effects of the SDF-1-CXCR4 axis in organogenesis, regeneration and tumorigenesis. Leukemia 20: 1915–1924.

Richter, R.P., Baranova, N.S., Day, A.J., and Kwok, J.C. (2018). Glycosaminoglycans in extracellular matrix organisation: are concepts from soft matter physics key to understanding the formation of perineuronal nets? Curr. Opin. Struct. Biol. 50: 65–74.

Rodríguez-Fuentes, D.E., Fernández-Garza, L.E., Samia-Meza, J.A., Barrera-Barrera, S.A., Caplan, A.I., and Barrera-Saldaña, H.A. (2021). Mesenchymal stem cells current clinical applications: a systematic review. Arch. Med. Res. 52: 93–101.

Romagnani, P., Lasagni, L., Annunziato, F., Serio, M., and Romagnani, S. (2004). CXC chemokines: the regulatory link between inflammation and angiogenesis. Trends Immunol. 25: 201–209.

Rubinstein, M. and Colby, R.H. (2003). *Polymer physics*. Oxford University Press, New York.

Sadir, R., Baleux, F., Grosdidier, A., Imberty, A., and Lortat-Jacob, H. (2001). Characterization of the stromal cell-derived factor-1α-heparin complex. J. Biol. Chem. 276: 8288–8296.

Sagaradze, G.D., Basalova, N.A., Efimenko, A.Y., and Tkachuk, V.A. (2020). Mesenchymal stromal cells as critical contributors to tissue regeneration. Front. Cell Dev. Biol. 8: 1–13.

Son, B.-R., Marquez-Curtis, L.A., Kucia, M., Wysoczynski, M., Turner, A.R., Ratajczak, J., Ratajczak, M.Z., and Janowska-Wieczorek, A. (2006). Migration of bone marrow and cord blood mesenchymal stem cells in vitro is regulated by stromal-derived factor-1-CXCR4 and hepatocyte growth factor-c-met axes and involves matrix metalloproteinases. Stem Cell. 24: 1254–1264.

Spiller, S., Panitz, N., Limasale, Y.D.P., Atallah, P.M., Schirmer, L., Bellmann-Sickert, K., Blaszkiewicz, J., Koehling, S., Freudenberg, U., Rademann, J., et al. (2019). Modulation of human CXCL12 binding properties to glycosaminoglycans to enhance chemotactic gradients. ACS Biomater. Sci. Eng. 5: 5128–5138.

Stappenbeck, T.S. and Miyoshi, H. (2009). The role of stromal stem cells in tissue regeneration and wound repair. Science 324: 1666–1669.

Stich, S., Haag, M., Häupl, T., Sezer, O., Notter, M., Kaps, C., Sittinger, M., and Ringe, J. (2009). Gene expression profiling of human mesenchymal stem cells chemotactically induced with CXCL12. Cell Tissue Res. 336: 225–236.

Thönes, S., Rother, S., Wippold, T., Blaszkiewicz, J., Balamurugan, K., Moeller, S., Ruiz-Gómez, G., Schnabelrauch, M., Scharnweber, D., Saalbach, A., et al. (2019). Hyaluronan/collagen hydrogels containing sulfated hyaluronan improve wound healing by sustained release of heparin-binding EGF-like growth factor. Acta Biomater. 86: 135–147.

Tsurkan, M.V., Chwalek, K., Prokoph, S., Zieris, A., Levental, K.R., Freudenberg, U., and Werner, C. (2013). Defined polymer-peptide conjugates to form cell-instructive starPEG-heparin matrices in situ. Adv. Mater. 25: 2606–2610.

Turnbull, J.E. (2018). Enhancing the glycosciences toolkit: new GAGs in the lineup. Nat. Methods 15: 867–868.

Vanden Berg-Foels, W.S. (2014). In situ tissue regeneration: chemoattractants for endogenous stem cell recruitment. Tissue Eng. B Rev. 20: 28–39.

Walkowiak, J.J., Ballauff, M., Zimmermann, R., Freudenberg, U., and Werner, C. (2020). Thermodynamic analysis of the interaction of heparin with lysozyme. Biomacromolecules 21: 4615–4625.

Weber, H.M., Tsurkan, M.V., Magno, V., Freudenberg, U., and Werner, C. (2017). Heparin-based hydrogels induce human renal tubulogenesis in vitro. Acta Biomater. 57: 59–69.

Xu, D., Arnold, K., and Liu, J. (2018). Using structurally defined oligosaccharides to understand the interactions between proteins and heparan sulfate. Curr. Opin. Struct. Biol. 50: 155–161.

Yan, D. and Lin, X. (2009). Shaping morphogen gradients by proteoglycans. Cold Spring Harb. Perspect. Biol. 1: a002493–a002493, https://doi.org/10.1101/cshperspect.a002493.

Yao, W., Chen, M., Dou, X., Jin, H., Zhang, X., Zhu, Y., Sha, M., Liu, Z., Meng, X., Zhang, L., et al. (2019). Unravel a neuroactive sHA sulfation pattern with neurogenesis activity by a library of defined oligosaccharides. Eur. J. Med. Chem. 163: 583–596.

Yu, S.R., Burkhardt, M., Nowak, M., Ries, J., Petráek, Z., Scholpp, S., Schwille, P., and Brand, M. (2009). Fgf8 morphogen gradient forms by a source-sink mechanism with freely diffusing molecules. Nature 461: 533–536.

Yu, Y., Wu, R.X., Gao, L.N., Xia, Y., Tang, H.N., and Chen, F.M. (2016). Stromal cell-derived factor-1-directed bone marrow mesenchymal stem cell migration in response to inflammatory and/or hypoxic stimuli. Cell Adhes. Migrat. 10: 342–359.

Ziarek, J.J., Veldkamp, C.T., Zhang, F., Murray, N.J., Kartz, G.A., Liang, X., Su, J., Baker, J.E., Linhardt, R.J., and Volkman, B.F. (2013). Heparin oligosaccharides inhibit chemokine (CXC motif) ligand 12 (CXCL12) cardioprotection by binding orthogonal to the dimerization interface, promoting oligomerization and competing with the chemokine (CXC motif) receptor 4 (CXCR4) N terminus. J. Biol. Chem. 288: 737–746.

Zieris, A., Dockhorn, R., Röhrich, A., Zimmermann, R., Müller, M., Welzel, P.B., Tsurkan, M.V., Sommer, J.U., Freudenberg, U., and Werner, C. (2014). Biohybrid networks of selectively desulfated glycosaminoglycans for tunable growth factor delivery. Biomacromolecules 15: 4439–4446.